

Article

# Encapsulation of Babchi Oil in cyclodextrin-Based Nanosponges: Physicochemical Characterization, Photodegradation and *In Vitro* Cytotoxicity Studies

Sunil Kumar<sup>1</sup>, Pooja Sihag<sup>2</sup>, Francesco Trotta<sup>3</sup>, Rekha Rao<sup>1,\*</sup>

<sup>1</sup> Department of Pharmaceutical Sciences, Guru Jambheshwar University of Science and Technology, Hisar-125001, Haryana, India. sunilkundu450@gmail.com; rekhaline@gmail.com

<sup>2</sup> Department of Biotechnology, Indian Institute of Technology, Roorkee, India. poojasihag1592@gmail.com

<sup>3</sup> Department of Chemistry, University of Torino, Turin, Italy. francesco.trotta@unito.it

\*Correspondence: e-mail: rekhaline@gmail.com; Mob No: +919991048560

**Abstract:** Babchi (*Psoralea corylifolia*) oil is an important essential oil used in several traditional medicines to cure various disorders. This phytotherapeutic agent possesses number of pharmacological activities including antibacterial, antifungal, antioxidant, anti-inflammatory, immunomodulatory and antitumor. However, volatile nature, poor stability and solubility of babchi oil (BO) restrict its pharmaceutical applications. Hence, the aim of the present work was to encapsulate this oil in  $\beta$ -cyclodextrin nanosponges (NS) in order to overcome above limitations. To fabricate nanosponges,  $\beta$ -cyclodextrin was crosslinked with diphenyl carbonate in different molar ratios *viz.* 1:2, 1:4, 1:6, 1:8 and 1:10. The blank nanosponges were loaded with babchi oil using freeze-drying method. Particle size of the babchi oil loaded nanosponges was found to lie between 200-500 nm, with low polydispersity index. Further, zeta potential, Fourier transform infrared spectroscopy, X-ray diffraction, thermal analysis and electron microscopy were carried out for characterization of babchi oil nanosponges. Results obtained from spectral analysis ascertained the formation of inclusion complexes. Additionally, solubilisation efficiency of the babchi oil was checked in distilled water and found enhanced by 4.95 times with optimized  $\beta$ -cyclodextrin nanosponges. The cytotoxicity study was carried out by MTT assay using HaCaT cell lines. A significant improvement in photostability of essential oil was also observed by inclusion in nanosponges. Lastly, the optimized formulation was tested for antibacterial activity using *Staphylococcus aureus*, *Pseudomonas aeruginosa* and *Escherichia coli*. Hence, encapsulation of BO in nanosponges resulted in efficacious carrier system in terms of solubility, photostability as well as safety of this oil along with handling benefits.

**Keywords:** Essential oil; *Psoralea corylifolia*; cytotoxicity; encapsulation; solubilisation.

## 1. Introduction

Encapsulation strategies play a vital role for the delivery of poorly soluble, unstable or toxic moieties. Enhancing their encapsulation efficiency using carrier systems can help in achieving better therapeutic efficacy with reduction in side effects. Hence, newer encapsulation techniques are explored using natural polymers, nowadays.

Naturally occurring polysaccharides act as attractive polymers for drug delivery systems due to their high biodegradability, biocompatibility and lower cost [1]. One of the most extensively used

natural polysaccharide includes cyclodextrins. Cyclodextrins possess the ability to encapsulate guest molecules inside their internal cavity leading to modification of the physico-chemical features of the host molecules like physical state, solubility, stability, and bioavailability [2, 3]. However, cyclodextrins are unable to form inclusion complexes with hydrophilic or high-molecular-weight molecules [4]. In the last few years, nanosponge has been proposed as an advanced drug delivery system involving reaction of cyclodextrin with suitable cross-linking agent, for encapsulation of difficult-to-formulate moieties [5-8]. These are hyper cross-linked nanoporous structures reported to form inclusion and non-inclusion complexes with variety of drugs to enhance their solubility, stability, permeability, cytotoxicity and other such drug delivery features [9].

Essential oils composed of lipophilic and highly volatile secondary plant metabolites, represent a "natural" alternative in pharmaceutical, cosmetic, food and agriculture fields due to their antiviral, antimicrobial, antifungal, insecticidal, nematocidal and antioxidant properties [10]. An important essential oil obtained from *Psoralea coryfolia* is babchi oil, a vital phytotherapeutic agent reported for treatment of psoriasis [11]. Antipsoriatic effect of babchi oil is attributed to psoralen, bakuchiol and isopsoralen content, which are the major constituents of this oil [11-12]. These chief constituents (furocoumarins) collectively inhibit DNA synthesis causing reduction in cell proliferation [13]. In addition, the babchi oil also possesses numerous activities like antifungal, antibacterial, antiviral, antitumor, cytotoxic, antioxidant, antidepressant and stimulant [11]. However, this essential oil is found to have poor aqueous solubility, stability and is volatile in nature [14]. These drawbacks limit the practical use of this oil, inspite of its numerous beneficial effects. Faiyazuddin *et al.*, fabricated and evaluated solid lipid nanoparticles of babchi oil. But poor stability, sterilization difficulties and low drug loading limits the use of solid lipid nanoparticles [15]. Unlike these, cyclodextrin nanosponges possess larger cavities for host molecules to be entrapped in the nano pores due to crosslinking network of polymer and crosslinker. In addition, these nano systems have also been proposed as stable carriers for entrapment of variety of therapeutic agents [16-19]. Although, various phytoconstituents like resveratrol [20],  $\gamma$ -oryzanol [18], curcumin [21], quercetin [19], rutin, phloridzin and chlorogenic acid [22] have been successfully encapsulated in cyclodextrin nanosponges, there are no reports on the encapsulation of essential oils using cyclodextrin nanosponges. Based on the above mentioned facts, the purpose of the present study was the evaluation of nanosponge as encapsulating agent for babchi essential oil found in *Psoralea coryfolia* seeds. In this preliminary investigation,  $\beta$ -CD nanosponges were purposely tailored for the formulation of this essential oil with poor water solubility. Prepared nanosponges may solubilise babchi oil by complexation and improve its stability. The physico-chemical characterization of the babchi oil nanosponge formulations was carried out by thermogravimetry analysis (TGA), X-ray powder diffraction (XRPD) and Fourier transform infra red (FTIR) spectroscopy. The fabricated NS were also characterized regarding topography and microstructure using field emission scanning electron microscopy (FE-SEM) and transmission electron microscopy (TEM). In addition, particle size analysis, zeta potential and polydispersity index were also investigated for babchi oil loaded nanoformulations. The safety of the optimized nanosponges was assessed by MTT assay using HaCaT (human epidermal keratinocyte) cell line. Further, *in vitro* antibacterial studies were explored to compare the antibacterial efficacy of the optimized nanosponges against plain babchi oil. The photodegradation of the babchi oil and babchi oil loaded nanosponges upon long UV irradiation were also carried out.

## 2. Experimental

### 2.1. Materials

The babchi oil was obtained as generous gift sample from Pukhraj Herbals, Mandsaur (India).  $\beta$ -cyclodextrin ( $\beta$ -CD) was procured from Jay Chem Marketing, Mumbai (India). Diphenyl carbonate (DPC) was purchased from Sigma-Aldrich (Milan, Italy). All other reagents and chemicals used were of analytical grade. Double distilled water was used throughout the studies.

## 2.2. Gas chromatography mass spectrometry of the babchi oil

Gas chromatography mass spectrometry (GC-MS) analysis was carried out using a GC-2010 gas chromatography (Shimadzu Corp., Kyoto, Japan) equipped with a GCMS-QP2010 Plus along with thermal desorption system TD 20 (Shimadzu Corp., Kyoto, Japan). Sample (0.2  $\mu$ l) was injected into the split injector with a split ratio of 1:100. Oven temperature was kept at 50 °C for 2 min, increasing to 210 °C at a rate of 3 °C/min and holding for 1 min, finally increasing to 280 °C at a rate of 8 °C/min and holding for 6 min. Injector temperature was 260 °C, while the ion source temperature and interface temperature were 230 °C and 270 °C, respectively. Identification of constituents was established on comparison of their mass spectra. The peak area measurement (expressed in area percentage) was used for quantitative analysis of each component of babchi oil.

## 2.3. Synthesis of nanosponges

Cyclodextrin-based nanosponges were prepared using previously reported procedure [23, 24]. Different molar ratios of  $\beta$ -CD and DPC (1:2, 1:4, 1:6, 1:8 and 1:10) were used for preparation of babchi oil nanocarriers.

Briefly, finely homogenized anhydrous  $\beta$ -CD and DPC were gradually heated to 90-100 °C under magnetic stirring for 6 hrs. Then, crystals of phenol formed at the neck of the flask were carefully removed. The reaction mixture was cooled to room temperature and the product was broken up roughly. The solid so obtained was repeatedly washed with distilled water in order to remove unreacted  $\beta$ -CD and subsequently extracted by soxhlet apparatus using acetone, to remove the unreacted DPC and phenol. After every washing, test for phenol was carried out using ferric chloride solution. The nanosponges thus, obtained were dried at 40 °C in hot air oven for 2 hrs and stored at room temperature in dessicator until further use [24].

## 2.4. Solubilization efficiency of nanosponges

In order to examine the solubilisation enhancement capacity, the solubilisation efficiency of the babchi oil in  $\beta$ -CD and all the batches of nanosponges (NS2, NS4, NS6, NS8 and NS10) were investigated [19, 21]. An excess amount of the babchi oil (50 mg) was taken with fixed amount (20 mg) of blank nanosponges in 20 ml of double distilled water in volumetric flask. The volumetric flasks were allowed to shake on a mechanical shaker at ambient temperature for 24 hrs. After equilibrium, the obtained suspensions were centrifuged at 10,000 rpm for 10 min to assort colloidal supernatant and free babchi oil. Dimethylsulfoxide (10 ml) was added to supernatants in order to extract the encapsulated babchi oil from the nanosponges. After 2 hrs, the colloidal supernatant solutions were examined by UV spectrophotometer (Varian Cary-5000) at 265 nm using calibration curve of babchi oil. The experiments were performed in triplicate.

## 2.5. Preparation of Babchi oil-loaded $\beta$ -cyclodextrin nanosponges

Babchi oil-loaded nanosponges (BONS) were prepared by freeze-drying technique as previously reported [25]. Accurately weighed quantities (1gm) of nanosponges were suspended in 50 ml of Milli-Q water using a magnetic stirrer, then excess amount of babchi oil was added, and the mixture was sonicated for 10 min and kept for 24 hrs under stirring. The suspensions were centrifuged at 3000 rpm for 10 min to separate the uncomplexed drug as a residue below the colloidal supernatant. The supernatant was freeze-dried using a lyophilizer (Alpha 2-4 LD Plus CHRIST) at -81 °C temperature and operating pressure 0.0010 mbar. The dried powder was stored in a desiccator. The drug-loaded NS formulations obtained were named as BONS2, BONS4, BONS6, BONS8, and BONS10 depending on ratio of  $\beta$ -CD and DPC used in fabrication of nanosponges [19].

## 2.6. Evaluation of nanosponges

### 2.6.1. Determination of the babchi oil content in the nanosponges

A weighed amount of all types of Babchi oil-loaded NSs was dispersed in dimethylsulfoxide (DMSO), sonicated for 10 min to break the nanosponge complex and diluted suitably using DMSO. Further, the prepared samples were analysed by UV spectrophotometer (Varian Cary -5000) at 265 nm to ascertain the drug content in nanosponges. The encapsulation efficiency and essential oil loading capacity were calculated using the following equations

$$\text{Drug loading}(\%) = \frac{\text{weight of essential oil in nanosponges}}{\text{weight of nanosponges}} \times 100 \quad 1$$

$$\text{Entrapment efficiency}(\%) = \frac{\text{weight of essential oil in nanosponges}}{\text{weight of essential oil feed initially}} \times 100 \quad 2$$

### 2.6.2. Determination of size, polydispersity index and zeta potential of the nanosponges

The size and polydispersity indices of the all NSs were determined by dynamic light scattering using a Malvern Zetasizer (Malvern Instruments Ltd, Worcestershire, UK). The samples were suitably diluted with filtered double distilled water before each measurement. Zeta potential measurements were made using an additional electrode in the same instrument. For the zeta potential determination, the instrument was operated at a constant temperature of 25 °C using a clear disposable zeta cell. Twelve measurements were carried out and their average was expressed.

**Based on the results of the encapsulation and solubilisation efficiency, formulation BONS4 was selected for further FTIR, TGA, XRPD, FE-SEM and TEM.**

### 2.6.3. Fourier transform infrared spectroscopy

Fourier transform infrared spectra were recorded in the spectral range of 4000-650 cm<sup>-1</sup> using a Perkin Elmer Spectrum, BX II instrument in the attenuated total reflectance (ATR) mode with a diamond crystal using 45 scans per spectrum and a resolution of 2 cm<sup>-1</sup>.

### 2.6.4. Thermal analysis

Thermal analysis was performed using EXSTAR TG/DTA 6300 (Thermo gravimetric/Differential Thermal Analyzer (TG/DTA) (SII 6300 EXSTAR)). A heating rate of 10 °C/min was employed in the 5-500 °C temperature range. The standard aluminium pans were used. Alumina powder was used as reference standard. About 10 mg of the sample was placed on the aluminium pan and subjected to the above mentioned program under a nitrogen atmosphere with 200 ml/min speed. Thermal analysis was performed to understand inclusion of babchi oil in nanosponges. The experiments were carried out in triplicate.

### 2.6.5. X-ray powder diffraction

In order to explore, the host-guest interaction and structure of the resulting nanocomplexes, X-ray powder diffraction study was carried out. Plain β-CD, plain DPC, blank nanosponges and babchi oil loaded nanosponges were subjected to XRPD using Powder X-ray Diffractometer (Bruker D8 Advance). Diffraction profiles were analysed at 2θ of 25 to 100° sequential collection. The step time was 0.5 second and time of acquisition was 1 hour.

### 2.6.6. Surface morphology

Field emission scanning electron microscopy

The morphology of the nanosponges and babchi oil-loaded nanosponges was observed under FE-SEM (Carl Zeiss UltraPlus). The samples were sprinkled on a double-sided carbon adhesive tape stuck to an aluminium stub, and then metallized with a thin film (10Å) of gold under an argon atmosphere for 90 sec to minimise the charging effects.

Transmission electron microscopy

The morphology of the blank nanosponges and BONS was also observed under TEM (FEI Tecnai G<sup>2</sup> 20 S-Twin, USA). One drop of formulation suspension was deposited on a carbon-coated copper grid and allowed to dry for contrast enhancement.

## 2.7. Cytotoxicity studies against HaCaT cell line

The cytotoxicity of the babchi oil and babchi oil loaded nanosponges were assessed using HaCaT cell lines. The HaCaT is a spontaneously transformed aneuploid immortal keratinocyte cell line from adult human skin [26]. These cell lines are used due to high tendency to differentiate and anti proliferate *in vitro* [27].

For cytotoxicity studies, the samples were weighed and mixed to obtain the desired concentration. The mixture was dissolved in distilled DMSO and volume was made up with Dulbecco's Modified Eagle's medium (DMEM) supplemented with 2 % inactivated Fetal Bovine Serum (FBS) to obtain a stock solution (1 mg/ml). After sterilization of stock solution by filtration, serial two fold dilutions (0-320 µg/ml) were prepared from it for carrying out cytotoxic analysis.

HaCaT cells were cultured in DMEM medium supplemented with 10% inactivated FBS, penicillin (100 IU/ml) and streptomycin (100 µg/ml) in a humidified atmosphere of 5% CO<sub>2</sub> at 37 °C until confluent. The cells were dissociated with TPVG solution (0.2 % trypsin, 0.02 % EDTA, 0.05 % glucose in PBS). Further, 50,000 cells / well of cells were seeded in a 96 well plate and incubated for 24 hrs at 37 °C, 5 % CO<sub>2</sub> incubator.

The monolayer cell culture was trypsinized and the cell count was adjusted to  $1.0 \times 10^5$  cells/ml using respective media containing 10% FBS. To each well (96 well microtiter plate), 100 µl of the diluted cell suspension (50,000 cells/well) was added. The plates were then incubated at 37 °C for 24 hrs in 5% CO<sub>2</sub> atmosphere. After incubation period, 3-[4, 5- dimethylthiazol-2-yl]-2, 5-diphenyl tetrazolium bromide (MTT) (5 mg/10 ml of MTT in PBS) was added to each well. After incubation of 4 hrs at 37 °C in 5% CO<sub>2</sub> atmosphere, the supernatant was removed. 100 µl of DMSO was added to the collected supernatant. The plates were read at 590 nm with a microplate reader (model 450). The percentage growth inhibition was determined and concentration of test drug needed to inhibit cell growth by 50% (IC<sub>50</sub> values) is generated from the dose-response curves.

## 2.8. Photodegradation study

The photodegradation of babchi oil and babchi oil-loaded nanosponges (BONS4) was carried out under UV lamp (Philips 40 W TL K05). Both samples were placed at 10 cm distance from the UV lamp for 60 minutes under dark. The samples were collected at time interval of 10 minutes and quantitatively analysed using UV spectrophotometer (Varian Cary-5000). The experiment was performed in triplicate.

## 2.9. Antibacterial activity

The antibacterial activity of the babchi oil, blank nanosponges, and babchi oil loaded nanosponges was evaluated by agar well diffusion method using nutrient agar medium. Nutrient agar medium (30 ml) was poured into each petri plate. The test bacteria i.e. *Staphylococcus aureus* ATCC 25923 (*S. aureus*), *Pseudomonas aeruginosa* ATCC 27853 (*P. aeruginosa*) and *Escherichia coli* ATCC



25922 (*E. coli*) ( $1 \times 10^6$  CFU/ml) were inoculated onto the surface of medium with a sterile spreader. Afterwards, the agar medium is punched using a cork borer (diameter 6 mm). BO loaded nanosponges (equivalent to 50 mg of BO) dispersion were pipetted into the wells. The antibiotic streptomycin (STP) (10  $\mu$ g/ml) was used as positive control. The plates were allowed to incubate at 37 °C for 24 hrs. The diameter of the growth inhibition of all the samples surrounding the wells was examined after incubation period. The experiment was repeated thrice and the antibacterial activity was calculated as average value [28].

## 2.10. Statistical analysis

All the experiments were performed in triplicate, and the results were reported as mean  $\pm$  standard deviation. Statistical measurements were carried out by GraphPad Prism version 5.01 software (GraphPad Software, Inc, USA). One-way Anova (non parametric) Kruskal wallis test was used to appraise the significant difference between results.

## 3. Results and discussion

Numerous efforts have been devoted to the method of preparation and application of nanosponges over the last decade. Amongst the various types of nanosponges, cyclodextrin based nanosponges have received more attention and are widely studied [29].

Cyclodextrins are biodegradable, versatile compounds used to improve physicochemical and pharmaceutical properties such as solubility, stability and bioavailability of administered drug molecules as reported in literature [30]. Among the natural ( $\alpha$ ,  $\beta$ ,  $\gamma$ ) cyclodextrins,  $\beta$ -cyclodextrin has the highest complexing ability and stability with cross-linking agents. Also, cavity dimensions, low cost of production and higher productive rates are other advantages offered by cyclodextrins for nanosponge preparation [31]. Various crosslinking agents like carbonyl diimidazole, hexamethylene diisocyanate, toluenyl dianhydride, diisocyanate or carbonate and diphenyl carbonate have been explored in literature for nanosponge formulations [6]. In the present work, diphenyl carbonate was chosen as cross-linker owing to its trifling acute dermal toxicity (2000 mg/kg), no skin irritancy, sensitization and minimum lineal photodegradation [32].

Nanosponges can be crafted using various techniques namely ultrasound-assisted synthesis [25], solvent evaporation technique [21], emulsion solvent diffusion method [33], microwave assisted synthesis [34], normal solution synthesis [35] and melt method [24].

In the present study, melt technique has been used for preparation of babchi oil cyclodextrin nanosponges. The advantage of using this technique is that it results in crystalline product without the use of organic solvents. Further, it has been revealed that the drug loading is greater in crystalline nanosponges in comparison to paracrystalline ones [36].

Aldawsari *et al.*, formulated and evaluated lemongrass oil-loaded ethylcellulose nanosponges using emulsion solvent evaporation technique [37]. However, cyclodextrin nanosponges have not been explored for encapsulating essential oils, yet these may prove as promising nanocarriers for these bioactives. Drug loading in cyclodextrin nanosponges is usually done at room temperature through freeze drying technique after fabrication of blank nanosponges. Hence, these nanocarriers may prove beneficial for essential oils which are generally thermolabile, volatile and poorly soluble. Thus, taking this into consideration, cyclodextrin nanosponges have been explored for encapsulation of babchi oil in the present investigation.

### 3.1. Identification of various compounds in babchi oil using GC-MS

Generally, the gas chromatography is applied for qualitative analysis while for quantitative estimation, it is coupled with mass spectrometry. In the present work, GC-MS was used to identify

the volatile components present in babchi oil sample. A large number of constituents were detected in this essential oil. Among them, bakuchiol (4-(3,7-Dimethyl-3-vinylocta-1,6-dien-1-yl)phenol) was evidenced as major component with the highest percentage area (65.37 %). Other main constituents included 2H-furo[2,3-H]-1-benzopyran-2-one (2.59 %), caryophyllene oxide (2.11 %), oleoyl chloride (1.70 %), 2-Phenyl-4-anilino-6[1H]-pyrimidinone (1.47 %), 9-Octadecenoic acid (1.29 %), 2-[5-(2-Methyl-benzooxazol-7-yl)-1H-pyrazol-3-yl]-phenol (1.11 %) and stigmast-5-en-3-ol (1.04 %). The rest of the volatile constituents were found at concentrations lower than 1% (caryophyllene, hexadecanoate, 2H-furo[2,3-H]-1-benzopyran-2-one, solanesol and stigmasterol).

3.2. Nanosponge fabrication

In the present study, the blank nanosponges were fabricated by melt method in five different molar concentrations (Table 1) using  $\beta$ -CD and DPC and their physico-chemical characterization was performed.

Table 1 Molar ratios of  $\beta$ -cyclodextrin and diphenyl carbonate (n=3, mean  $\pm$  SD).

Sr. no.	Nanosponge type	Molar ratio $\beta$ -CD : DPC	Amount of $\beta$ -CD (g)	Amount of DPC (g)	Practical yield (g) $\pm$ SD
1	NS2	1:2	4.548	1.712	3.544 $\pm$ 0.220
2	NS4	1:4	4.548	3.424	4.559 $\pm$ 0.199
3	NS6	1:6	4.548	5.136	5.896 $\pm$ 0.197
4	NS8	1:8	4.548	6.848	6.434 $\pm$ 0.197
5	NS10	1:10	4.548	8.56	6.735 $\pm$ 0.296

Statistical analysis from Kruskal-Wallis test (practical yield: Kruskal-Wallis statistics – 13.23) with  $p < 0.05$ .

The molar ratio ( $\beta$ -CD : DPC) used in nanosponges was found to affect their practical yield. It has been observed that the practical yield increased with increase in the molar ratio. This may be due to increase in number of reactive functional groups at higher concentrations.

3.3. Solubilization efficiency of nanosponges

The solubilisation capacity of  $\beta$ -CD and all the prepared nanosponges for babchi oil was evaluated and compared with the solubility of the free babchi oil in double distilled water. All the five types of nanosponges (NS2 – NS10) enhanced the solubility of the babchi oil in comparison to free babchi oil as shown in Figure 1 (Kruskal-Wallis statistics - 15.10 with  $p < 0.05$ ). Among all, NS4 showed maximum solubilisation efficiency (1105  $\mu$ g/ml) followed by NS6 (1030  $\mu$ g/ml), in comparison with free babchi oil (223.2  $\mu$ g/ml). With plain  $\beta$ -CD, free babchi oil exhibited solubilisation efficiency (851.1 $\mu$ g/ml). Here, solubilisation efficiency data depicted the superiority of  $\beta$ -CD nanosponges over plain  $\beta$ -CD. The formation of inclusion complex with the babchi oil as well as encapsulation in nanosponge matrix may have resulted in enhanced solubilisation of this oil. This observation demonstrated that encapsulation of babchi oil in nanosponges resulted in the solubility enhancement of this essential oil. However, low solubilisation efficiency of NS2, NS8 and NS10 was observed in comparison to plain  $\beta$ -CD for babchi oil. In NS2, the degree of cross-linking may be low resulting in insufficient nanochannels which do not have a remarkable impact on the solubility of free babchi oil. Whereas, in NS8 and NS10 formulations, higher degree of cross-linking created more tortuous and complex nanochannels, leading to prevention of the entrapment of babchi oil into the NS structures. Anandam and Selvamuthukumar reported that solubilisation of quercetin in milli-Q water was enhanced by 20 times using  $\beta$ -CD and DPC as crosslinker [19].

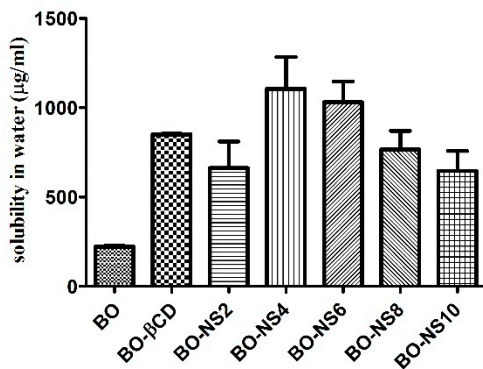


**Fig. 1** Solubilization of babchi oil by nanosponges (having different cross-linking density) and  $\beta$ -CD.

**3.4. Loading and encapsulation efficiency**

Babchi oil was loaded into all the five types of nanosponges by freeze drying technique. Figure 2 indicates loading efficacy of babchi oil by NS in different molar ratios. Among the five types of nanosponge, the loading efficiency was observed to be higher in BONS4 (1:4) as much as 21.47 % w/w followed by BONS6 (20.44 %) > BONS2 (19.75 %) > BONS8 (14.53 %) > BONS10 (14.23 %). The results revealed that the degree of cross-linking affected the complexation efficiency of nanosponges. It was found that at 1:2 molar ratio, the degree of cross-linking may be low, resulting in insufficient nanochannels for the guest complexation; thus babchi oil might not be encapsulated in higher amounts. While in BONS6, BONS8 and BONS10, the higher amount of cross-linker resulted in hyper cross-linking of  $\beta$ -CD, leading to hindrance in interaction of babchi oil with  $\beta$ -CD cavities. The encapsulation efficiencies of BONS formulations were found to be 61- 93 % (Table 2).

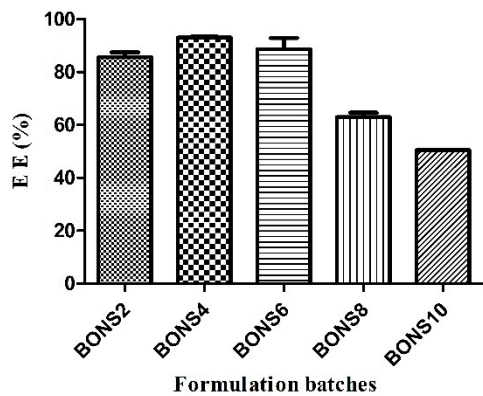


**Fig. 2** Encapsulation efficiency of the nanosponges (NS2-NS10).

**Table 2** Particle sizes, zeta potentials, poly dispersity index and % encapsulation efficiency of the babchi oil formulations (n=3, mean  $\pm$  SD).

Sr. No.	Formulation	Particle size (nm $\pm$ SD)	Zeta potential (mV $\pm$ SD)	Poly dispersity index $\pm$ SD	% Encapsulation efficiency $\pm$ SD
1.	BONS1:2	261.6 $\pm$ 14.79	-17.8 $\pm$ 2.52	0.312 $\pm$ 0.098	85.61 $\pm$ 1.848
2.	BONS1:4	360.9 $\pm$ 11.55	-16.0 $\pm$ 1.15	0.311 $\pm$ 0.059	93.05 $\pm$ 0.283
3.	BONS1:6	234.3 $\pm$ 15.37	-15.5 $\pm$ 1.17	0.188 $\pm$ 0.064	88.61 $\pm$ 4.286
4.	BONS1:8	484.2 $\pm$ 19.89	-15.6 $\pm$ 2.39	0.509 $\pm$ 0.236	62.98 $\pm$ 1.669
5.	BONS1:10	243.3 $\pm$ 12.95	-22.0 $\pm$ 2.47	0.361 $\pm$ 0.113	50.43 $\pm$ 0.173

Statistical analysis from Kruskal-Wallis test (encapsulation efficiency: Kruskal-Wallis statistics -16.97) with  $p < 0.01$ .



The encapsulation efficiency of entire formulations followed order: BONS4>BONS6>BONS2>BONS8>BONS10 as shown in **Figure 2**. It was found that for the babchi oil NS, encapsulation efficiency was highest in BONS4 as much as 93 %, while 61 % in BONS10. The reason for more encapsulation of the babchi oil in 1:4 molar ratio may be optimum crosslinking, involving inclusion and external interactions, at the same time which provides more quantity of oil to encapsulate in the nanosponge matrix as well as cyclodextrin cavity. The effect of  $\beta$ -CD and crosslinker ratio on entrapment efficiency of  $\beta$ -CD based nanosponges has been extensively reported [38].

### 3.5. Particle size, Polydispersity index and zeta potential determination

The particle size of the babchi oil nanosponges ranged from 234-484 nm as presented in **Table 2**. All the prepared babchi oil nanosponges depicted particle size in nano range ( $< 1\mu\text{m}$ ). Zeta potential of different babchi oil nanoformulations was also checked, as a measure of surface charge. The results of zeta potential obtained are presented in **Table 2**. High zeta potential shows that the nanosponge would be stable due to higher magnitude of repulsive forces, leading to reduction in their tendency to aggregate. Reduced values of PDI with narrow range showed that the nanocolloidal suspensions are stable and homogenous in nature. All the prepared nanoformulations were found as fine and free flowing powders.

**Based on the results of the encapsulation and solubilisation efficiency, formulation BONS4 was selected for further characterization through FTIR, TGA, XRPD, FE-SEM and TEM.**

### 3.6. Fourier transform infrared spectroscopy

The babchi oil, blank nanosponges and babchi oil loaded nanosponges were subjected to FTIR analysis. The FTIR spectrum of the babchi oil showed characteristic absorption bands at around 3419, 2929, 1740, 1612, 1514, 1456, 1377, 1169 and 724  $\text{cm}^{-1}$ .

Plain NS exhibited a characteristic peak around 1777  $\text{cm}^{-1}$  due to carbonate bond and 3368  $\text{cm}^{-1}$  due to O-H stretching vibration, confirming the formation of CD based nanosponges. Additionally, other prominent peaks of NS were found at 2926  $\text{cm}^{-1}$  due to C-H stretching vibration, 1419  $\text{cm}^{-1}$  due to C-H bending vibration and 1029  $\text{cm}^{-1}$  due to C-O stretching vibration of primary alcohol. FTIR spectrum of  $\beta$ -CD (starting material for NS synthesis) showed no peak around 1700  $\text{cm}^{-1}$ , hence, ascertaining the formation of carbonate bond after their interaction with cross-linker (DPC) in nanosponges.

The comparison of FTIR spectra of babchi oil, blank NS and babchi oil loaded nanosponges evidenced that the characteristic peaks of the babchi oil were broadened or shifted in nanoformulations suggesting interactions between oil and nanosponges (**Figure 3**).

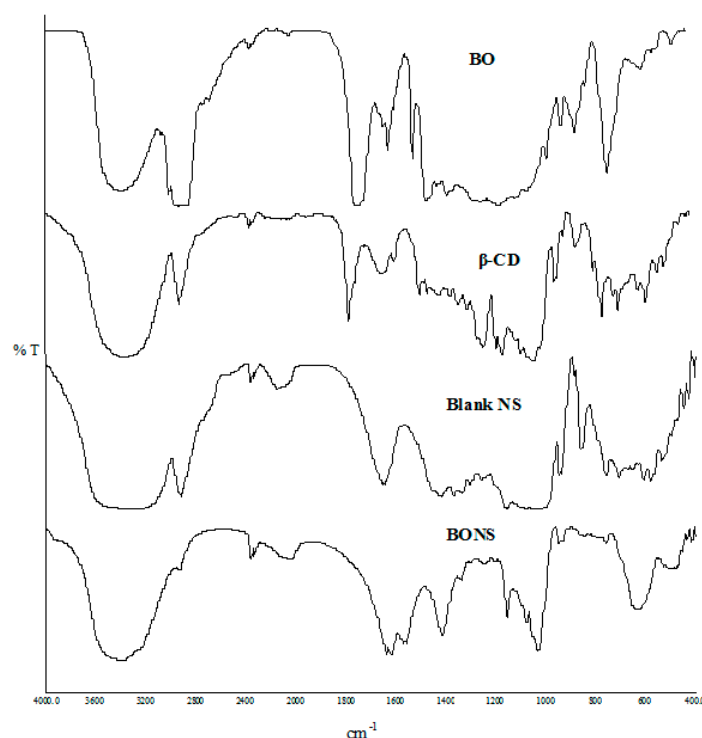


Fig. 3 FTIR spectra of Babchi oil,  $\beta$ -CD, blank NS and BONS4.

### 3.7. Thermal analysis

Thermo gravimetry analysis is an efficient way to examine alterations in chemical and physical properties of materials. Thermal analysis of  $\beta$ -CD, DPC, blank NS and their complexes ascertained not only presence of an inclusion compound but also a physical mixture of  $\beta$ -CD and DPC. **Figure 4 and 5** depicted the results of TGA and their derivatives (DTG) for  $\beta$ -CD, DPC, blank NS and BONS4, respectively.

On one hand, pure  $\beta$ -CD suffers a first weight loss (13.8 %) at 112 °C which is relating to evaporation of water associated with polymer ( $\beta$ -CD). The second zone around 300-337 °C with 53.7 % weight loss can be attributed to degradation of the  $\beta$ -CD. The third zone of weight loss (27.9 % to 16.8 %) from 337-438 °C can be assigned to char degradation. On the other, DPC showed weight loss (96.2 %) at 229 °C indicating its complete degradation. In case of the babchi oil nanosponges, the absence of the free babchi oil was revealed, and a slight shift of peaks was observed in the blank nanosponges.

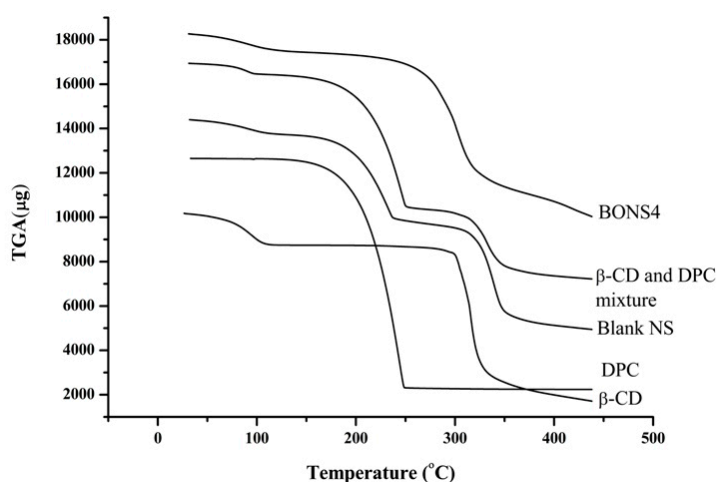
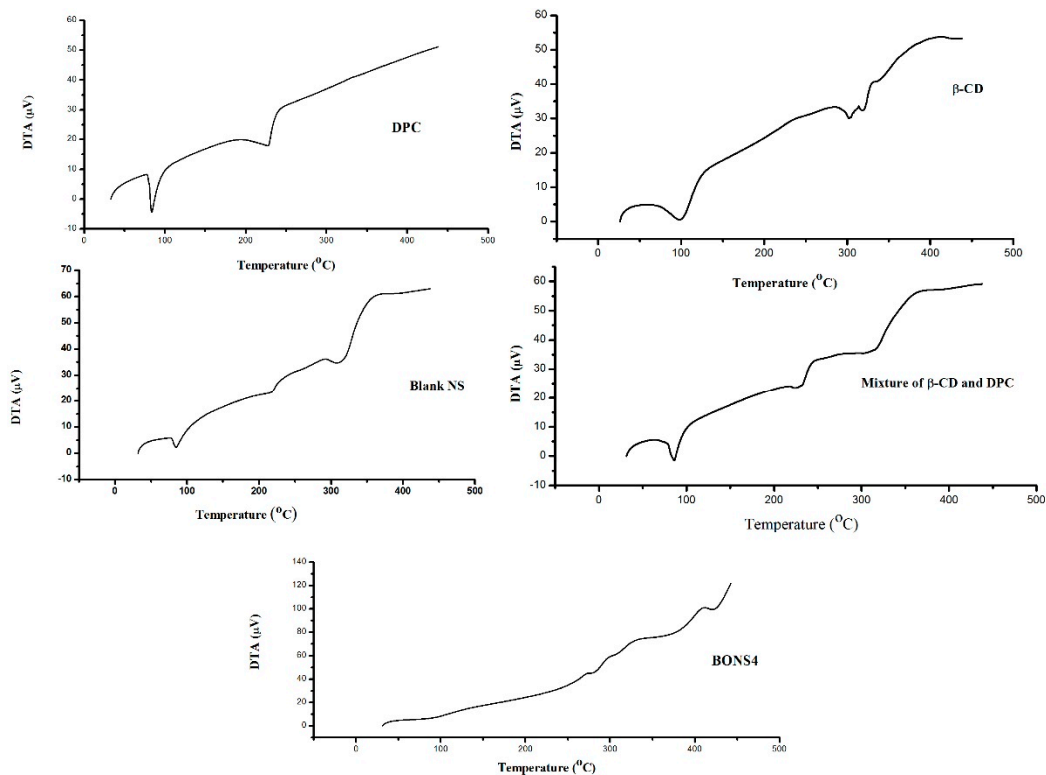


Fig. 4 TGA thermograms of  $\beta$ -CD, DPC, blank NS,  $\beta$ -CD and DPC mixture, and BONS4.



**Fig. 5** DTG thermograms of  $\beta$ -CD, DPC, blank NS, mixture of  $\beta$ -CD and DPC, and BONS4.

TGA curve of the  $\beta$ -CD and DPC mixture showed some similarity with blank nanosponges, ascertaining the some degree of crosslinking between polymer and DPC with increase in temperature. The peak below 100 °C is associated with residual moisture in the respective sample. However, for all nanosponges, maximum degradation processes of their crosslinked structures occur at 240-300 °C, indicating good thermal stability. DTG results helped in further strengthening the TGA findings (Table 3).

**Table 3** Derivative thermogravimetric analysis of the fabricating materials and nanosponges.

Formulating materials and NS	Derivative thermo gravimetric parameters		
	Tempearture (°C)	Type of peak	Derivative of thermo gravimetry (mg/min)
$\beta$ -CD	98	Exothermic	0.30
	304	Exothermic	1.54
DPC	317	Exothermic	3.26
	226	Sharp exothermic	2.69
$\beta$ -CD and DPC mixture	80	Exothermic	0.14
	231	Sharp exothermic	1.57
	315	Exothermic	0.88
Blank NS	217	Exothermic	0.96
	323	Exothermic	1.57
BONS4	272	Exothermic	0.76
	291	Exothermic	1.31

Differential thermal analysis measures the temperature difference between sample and reference, resulting in heat absorption or liberation. As shown in Figure 6, absence of characteristic peak of babchi oil in BONS4, indicated the inclusion complex formation in nanosponges. As indicated in Table 4, these results corroborate the previous findings of thermal analysis of the nanosponges.

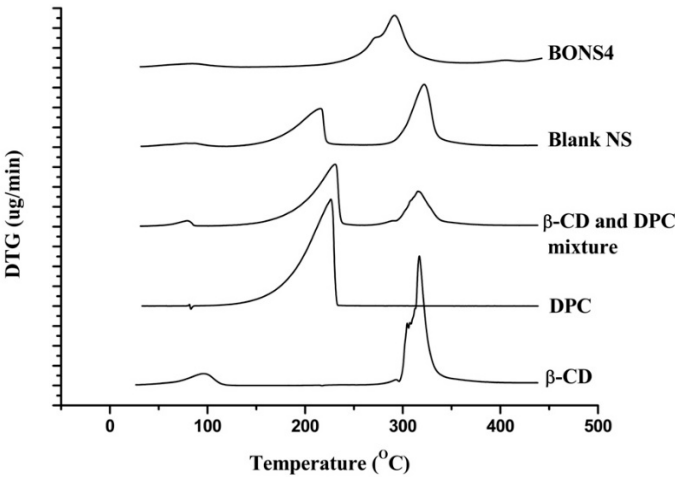


**Fig. 6** DTA thermograms of  $\beta$ -CD, DPC,  $\beta$ -CD and DPC mixture, blank NS and BONS4.

**Table 4** Differential thermal analysis of the fabricating materials and nanosponges.

Formulating materials and NS	Parameters of differential thermal analysis				DTA sensitivity ( $\mu$ V)
	Temperature ( $^{\circ}$ C)	Type of peak	Change Enthalpy mJ/mg	in ( $\Delta$ H)	
$\beta$ -CD	98	Endothermic	224	0.60	
	302	Endothermic	110	30.00	
	320	Endothermic	110	32.51	
DPC	83	Endothermic	96.20	-4.30	
	228	Endothermic	146	17.88	
$\beta$ -CD and DPC mixture	86	Endothermic	108	-1.50	
	231	Endothermic	49.50	24.30	
	317	Endothermic	160	37.00	
Blank NS	85	Endothermic	36.6	2.30	
	218	Endothermic	35.30	23.40	
	314	Endothermic	189	35.30	
BONS4	-	-	-	-	-

**3.8. X-ray powder diffraction**

Diffraction pattern of blank nanosponges and babchi oil loaded nanosponges (BONS4) has been showed in **Figure 7**. A significant difference between their diffractogram i.e. reduction in intensity of peaks was observed. Hence, the XRPD studies indicated that after freeze drying (BONS4), a fluffy powder was obtained having highly porous structure losing all its crystallinity. The characteristic peaks of the blank nanosponges were observed at 25.32°, 26.06°, 29.20°, 31.17°, 35.04°, 37.96° and 39.18° (2 $\theta$ ) as indicated in **Figure 7** and the intensity of these peaks were weakened in the babchi oil loaded nanosponges (**Figure 7**) confirming encapsulation of oil.

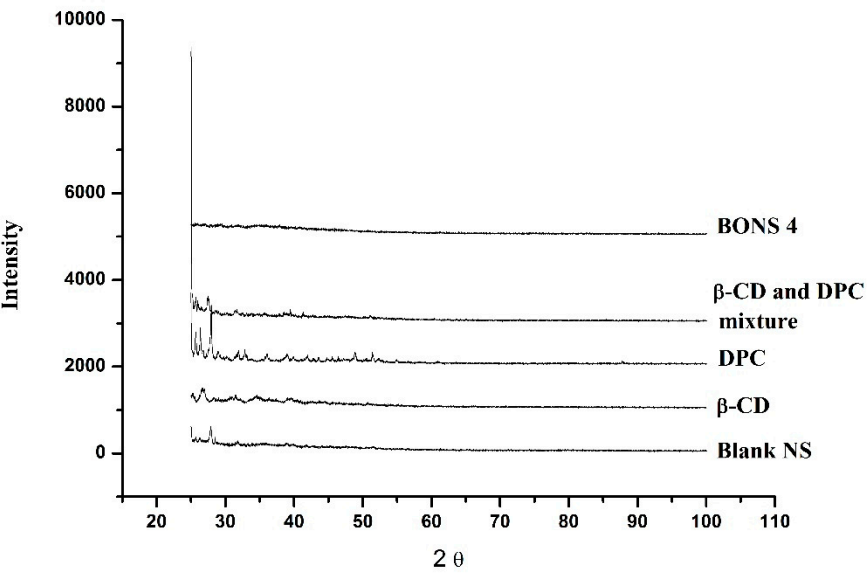


Fig. 7 XRPD patterns of β-CD, DPC, blank NS, β-CD and DPC mixture, and BONS4.

3.9. Surface morphology

The surface topography of the prepared nanosponges was also studied using scanning electron microscopy. As observed in FE-SEM images (Figure 8), cyclodextrin nanosponges showed crystalline morphologies. Additionally, the morphology of the selected babchi oil nanosponges (BONS4), and blank nanosponges was studied by transmission electron microscopy. Using TEM, a single crystal of nanosponge can be focused elucidating its definite crystalline geometry. As shown in representative TEM photographs (Figure 9), the dimensions of the crystal lattice agreed well with XRPD findings. The morphological characterization by this microscopy showed that the nanosponges prepared by melt method possess uniform size distribution, crystallinity and porous nature. Further, lattice planes lay straight across the nanosponges indicated that the obtained nanosponges possess high degree of crystallinity.

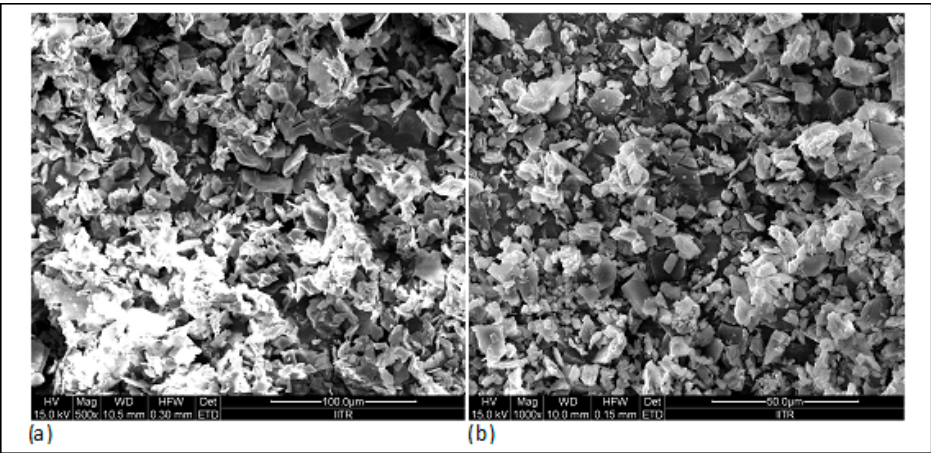
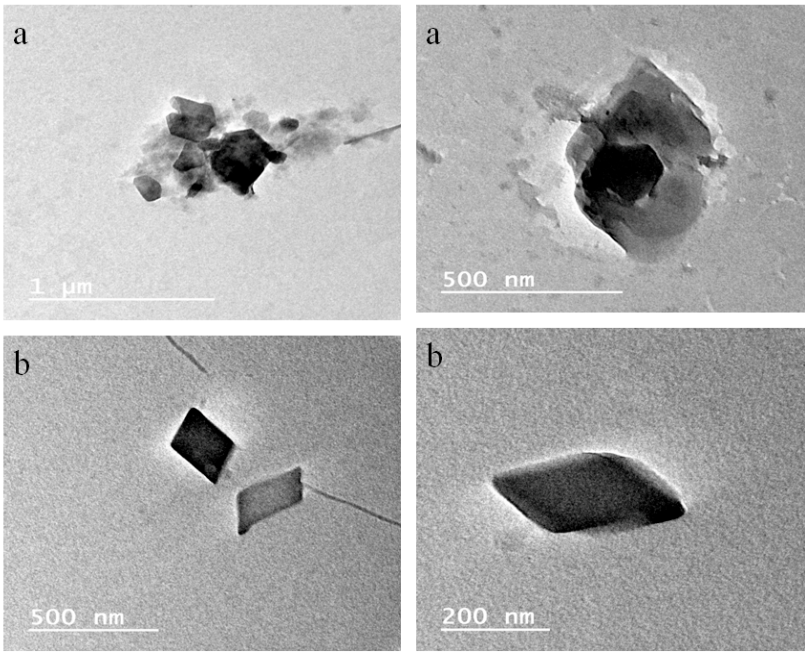


Fig. 8 Field emission scanning electron microscopy: a. plain NS; b. BONS4.





**Fig. 9** TEM images of a. blank nanosponges b. BONS4.

**3.10. Cytotoxicity studies against HaCaT cell lines**

Most of the essential oils have been reported to produce toxicity or skin irritation in spite of their good topical advantages. To compare the cytotoxicity of plain babchi oil and babchi oil loaded nanosponges, the dose response curve was established. Results indicated that cytotoxicity of the BONS was slightly less than that of BO. Hence, in order to explore the potential benefits of BO loaded nanosponges on human keratinocytes, the cytotoxicity of BO and BO loaded nanosponges were studied using MTT assay and the results of human skin cells treated with their different concentrations are presented in **Table 5**.

**Table 5** Effect of BO and BONS on viability of HaCaT cells as a function of the drug concentration at 24 h.

Sample	Concentration $\mu\text{g/ml}$	% inhibition $\pm$ standard deviation (n=3)	IC50
Control	0	0.00 $\pm$ 0.00	
Babchi oil	10	4.41 $\pm$ 1.21	172.3 $\mu\text{g/ml}$
	20	7.48 $\pm$ 1.47	
	40	16.84 $\pm$ 1.40	
	80	23.45 $\pm$ 1.20	
	160	38.61 $\pm$ 2.16	
	320	51.16 $\pm$ 2.23	
Babchi oil loaded nanosponges	10	4.26 $\pm$ 1.96	191.4 $\mu\text{g/ml}$
	20	9.60 $\pm$ 1.63	
	40	16.39 $\pm$ 1.74	
	80	25.86 $\pm$ 2.29	
	160	48.73 $\pm$ 2.09	
	320	61.27 $\pm$ 1.06	

Both these samples resulted in dose dependent reductions in cellular viability. Further, the MTT assay showed that the treatment of these cells with BO loaded nanosponges at 320  $\mu\text{g/ml}$  resulted in cytotoxic effect with IC50 value 191.4  $\mu\text{g/ml}$  and plain BO with IC50 value 172.3  $\mu\text{g/ml}$ . However, there is no significant difference between the cytotoxicity caused by BO and BONS, indicating that sufficient quantity of drug is released from nanosponges to cause cell toxicity. Hence, the results of

MTT assay indicated that the developed nanoformulation is safer on human skin cells in comparison to babchi essential oil (Table 5).

3.11. Photodegradation study

BO gets absorbed in the UV region exhibiting a peak around 265 nm. The intensity of this peak was found diminished upon UVA illumination ascertaining photolysis of babchi oil constituents.

With the objective to evaluate the protective phenomenon of nanosponges on the photodegradation of the babchi oil constituents, the photodegradation kinetics of this oil and oil-loaded nanosponges was also compared [18, 39, 40].

The BO concentration was plotted as a function of irradiation time to analyse the photodegradation kinetics. The obtained exponential asymptotic curve of the degraded BO upon BO irradiation followed first order kinetics. The following logarithmic equation was used for calculation of the slope of the obtained curves.

$$\ln C_t/C_0 = -k \times t$$

where  $C_0$  is the initial concentration of babchi oil,  $C_t$  represents its residual concentration at time  $t$ . Rate constant data can be calculated using the linear dependence of  $\ln C_t/C_0$  vs time. The  $k$  values were calculated using the pseudo-first order model fitting (Table 6).

Table 6 Correlation coefficient ( $r^2$ ) and rate constant ( $k$ ) of BO and BONS4 photodegradation under UVA irradiation.

Sr. No.	Oil and its formulation	Correlation coefficient ( $r^2$ )	Rate constant ( $k$ ) ( $1 \times 10^3 \text{ min}^{-1}$ )
1.	BO	0.968±0.10	39.151±0.76
2.	BONS4	0.978±0.12	2.303±0.59

A comparison of rate constants of photodegradation exhibited by BO ( $39.151 \times 10^3 \pm 0.76 \text{ min}^{-1}$ ) and BO loaded nanosponges ( $2.303 \times 10^3 \pm 0.59 \text{ min}^{-1}$ ) advocated that BO loaded nanosponges are capable to retard photooxidation process owing to the physical barrier provided by nanosponges against UV-induced oxidation of BO.

3.12. Antibacterial activity

Babchi oil loaded nanosponges showed a clear inhibitory effect against *P. aeruginosa*, *E. coli* and *S. aureus*. Although, babchi essential oil also exhibited an inhibitory effect, the antibacterial effect was significantly ( $p < 0.05$ ) improved for babchi oil loaded nanosponges. Zone of growth inhibition for babchi oil were as follows: 12.33 mm  $\pm$  2.5 for *S. aureus*, 12 mm  $\pm$  2.4 for *E. coli*, 12.33 mm  $\pm$  2.3 for *P. aeruginosa* while in BONS dispersion, it was 16.00 mm  $\pm$  2.64 for *S. aureus*, 17 mm  $\pm$  3.00 for *E. coli*, 16 mm  $\pm$  0.00 for *P. aeruginosa* (Figure 10). The positive control streptomycin (10  $\mu\text{g/ml}$ ) produced comparable zone of growth inhibition against *S. aureus* (10.00 mm  $\pm$  1.00), *E. coli* (16 mm  $\pm$  1.00 for), *P. aeruginosa* (15.33 mm  $\pm$  2.51) whereas negative control (blank nanosponge dispersion) plates did not showed growth inhibition of the above mentioned bacteria. The restraining antibacterial effects of babchi oil against *P. aeruginosa*, *E. coli* and *S. aureus* can be assigned due to water insolubility and volatile nature of oil. As observed from solubility studies, the entrapment of the BO in cyclodextrin nanosponges potentially improved the water solubility which might have resulted in enhancement of antibacterial activity.

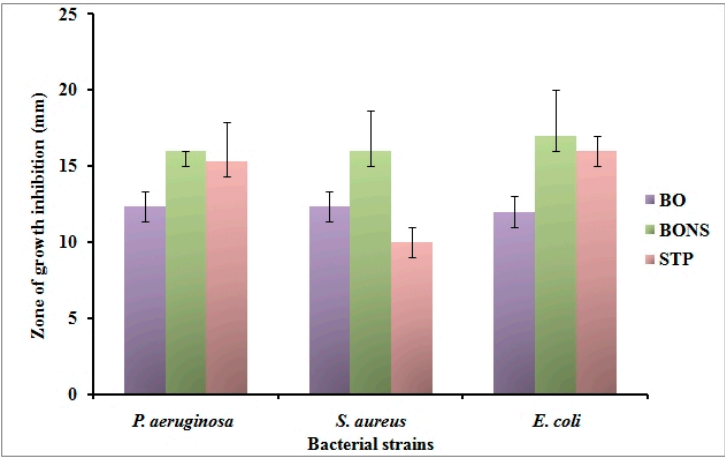


Fig.10 Antibacterial Activities of *Psoralea corylifolia* seed oil.

4. Conclusions

The present study reports encapsulation of babchi essential oil in  $\beta$ -cyclodextrin nanosponges. Firstly, GCMS analysis of babchi oil was performed in order to identify the compounds present in it. Solubilization studies showed all five types of fabricated nanosponges enhanced the solubility of babchi oil in comparison to free babchi oil. However, BONS4 exhibited highest solubilisation which can be attributed to the presence of babchi oil in nanochannels. For oil loading, babchi oil was efficiently impregnated onto carbonyl diphenylcarbonate cross-linked  $\beta$ -cyclodextrin nanosponges using freeze drying technique. Results of the encapsulation efficiency implies that an optimum ratio of the polymer to crosslinker in babchi oil nanosponges is 1:4 (molar ratio) and the product processed from this ratio can help in delivering therapeutically effective dose. Spectral characterization data revealed the formation of stable inclusion complexes in nanosponges. All characterization findings indicated that the essential oil is successfully encapsulated within the matrix of cyclodextrin complexes. The prepared nanosponges displayed significant oil entrapment and thermal stability. Cytotoxicity studies explored the enhancement in therapeutic response that will retard the overall drug consumption and dose, will minimize systemic side effects due to drug localization at target site. On the basis of calculated kinetic parameters, the nanosponges complexation minimises the UV photodegradation. The fabricated optimized formulation was found to be active on bacteria such as *P. aeruginosa*, *E. coli* and *S. aureus*, compared with pure essential oil. Further, research on pharmacological evaluation of babchi oil nanosponges is in progress. It will be helpful to explain the potential of babchi oil nanosponges for therapeutic applications.

Acknowledgements

The researchers would like to acknowledge the coordinator, DST-FIST, Department of Pharmaceutical Sciences, Guru Jambheshwar University of Science and Technology, Hisar for carrying out the zeta potential and particles size analysis. Pukhraj Herbals, Mandsaur and Jay Chem Marketing, Mumbai is to be thanked for providing a gift sample of babchi oil and  $\beta$ -cyclodextrin.

Conflict of interest

Authors declare no conflict of interest.

References

1. Rossi S, Ferrari F, Bonferoni MC, Caramella C. Characterization of chitosan hydrochloride–mucin interaction by means of viscosimetric and turbidimetric measurements. *Eur J Pharm Sci.* 2000;10(4):251-7.

2. Munin A, Edwards-Lévy F. Encapsulation of natural polyphenolic compounds; a review. *Pharmaceutics*. 2011;3(4):793-29.
3. Wadhwa G, Kumar S, Chhabra L, Mahant S, Rao R. Essential oil–cyclodextrin complexes: an updated review. *J Incl Phenom Macrocycl Chem*. 2017; 1-20.
4. Szejtli J. Cyclodextrin in drug formulations Part I. *Pharm Technol Int*. 1991; 3:15–22
5. Cavalli R, Trotta F, Tumiatti W. Cyclodextrin-based nanosponges for drug delivery. *J Incl Phenom Macrocycl Chem*. 2006;56(1-2):209-13.
6. Trotta F, Zanetti M, Cavalli R. Cyclodextrin-based nanosponges as drug carriers. *Beilstein J Org Chem*. 2012;8(1):2091-9.
7. Trotta F, Dianzani C, Caldera F, Mognetti B, Cavalli R. The application of nanosponges to cancer drug delivery. *Expert Opin Drug Deliv*. 2014;11(6):931-41.
8. Swaminathan S, Cavalli R, Trotta F. Cyclodextrin-based nanosponges: a versatile platform for cancer nanotherapeutics development. *Wiley Interdiscip Rev Nanomed Nanobiotechnol*. 2016; 8(4): 579-601.
9. Deshmukh K, Tanwar YS, Shende P, Cavalli R. Biomimetic estimation of glucose using non-molecular and molecular imprinted polymer nanosponges. *Int J Pharm*. 2015; 494(1): 244-8.
10. Turek C, Stintzing FC. Stability of essential oils: a review. *Compr Rev Food Sci Food Saf*. 2013;12:40-53.
11. Chopra B, Dhingra AK, Dhar KL. *Psoralea corylifolia* L.(Buguchi)—folklore to modern evidence: review. *Fitoterapia*. 2013;90:44-56.
12. Kumar S, Rao R. Psoralen: A promising boon in topical manifestations. *IJP*. 2016; 3(9): 375-383.
13. Chang L. Psoriasis Phototherapy: UVA Beats UVB. *WebMD Medical News* Daniel De Noon. 2006.
14. Musthaba SM, Baboota S, Ahmed S, Ahuja A, Ali J. Status of novel drug delivery technology for phytotherapeutics. *Expert Opin. Drug Deliv*. 2009;6(6):625-37.
15. Pradhan M, Singh D, Singh MR. Novel colloidal carriers for psoriasis: current issues, mechanistic insight and novel delivery approaches. *J Control Release*. 2013;170(3):380-95.
16. Mognetti B, Barberis A, Marino S, Berta G, De Francia S, Trotta F, Cavalli R. In vitro enhancement of anticancer activity of paclitaxel by a Cremophor free cyclodextrin-based nanosponge formulation. *J Incl Phenom Macrocycl Chem*. 2012;74(1-4):201-10.
17. Tejashri G, Amrita B, Darshana J. Cyclodextrin based nanosponges for pharmaceutical use: A review. *Acta Pharm*. 2013; 63(3):335-58.
18. Sapino S, Carlotti ME, Cavalli R, Ugazio E, Berlier G, Gastaldi L, Morel S. Photochemical and antioxidant properties of gamma-oryzanol in beta-cyclodextrin-based nanosponges. *J Incl Phenom Macrocycl Chem*. 2013;75(1-2):69-76.
19. Anandam S, Selvamuthukumar S. Fabrication of cyclodextrin nanosponges for quercetin delivery: physicochemical characterization, photostability, and antioxidant effects. *J Mater Sci*. 2014; 49(23):8140-53.
20. Ansari KA, Vavia PR, Trotta F, Cavalli R. Cyclodextrin-based nanosponges for delivery of resveratrol: in vitro characterisation, stability, cytotoxicity and permeation study. *AAPS PharmSciTech*. 2011;12(1):279-86.
21. Darandale SS, Vavia PR. Cyclodextrin-based nanosponges of curcumin: formulation and physicochemical characterization. *J Incl Phenom Macrocycl Chem*. 2013;75(3-4):315-22.
22. Ramírez-Ambrosi M, Caldera F, Trotta F, Berrueta LÁ, Gallo B. Encapsulation of apple polyphenols in  $\beta$ -CD nanosponges. *J Incl Phenom Macrocycl Chem*. 2014;80(1-2):85-92.
23. Rao M, Bajaj A, Khole I, Munjapara G, Trotta F. In vitro and in vivo evaluation of  $\beta$ -cyclodextrin-based nanosponges of telmisartan. *J Incl Phenom Macrocycl Chem*. 2013;77(1-4):135-45.
24. Rao MR, Shirsath C. Enhancement of Bioavailability of Non-nucleoside Reverse Transcriptase Inhibitor Using Nanosponges. *AAPS PharmSciTech*. 2016: 1-1.

- 543 25. Swaminathan S, Vavia PR, Trotta F, Cavalli R, Tumbiolo S, Bertinetti L, Coluccia S. Structural  
544 evidence of differential forms of nanosponges of beta-cyclodextrin and its effect on  
545 solubilization of a model drug. *J Incl Phenom Macrocycl Chem*. 2013;76(1-2):201-11.
- 546 26. Boukamp P, Petrussevska RT, Breitkreutz D, Hornung J, Markham A, Fusenig NE. Normal  
547 keratinization in a spontaneously immortalized aneuploid human keratinocyte cell line. *J*  
548 *Cell Biol*. 1988; 106: 761-771.
- 549 27. Schürer N, Köhne A, Schliep V, Barlag K, Goerz G. Lipid composition and synthesis of  
550 HaCaT cells, an immortalized human keratinocyte line, in comparison with normal human  
551 adult keratinocytes. *Exp Dermatol*. 1993; 2: 179-185.
- 552 28. Borate A, Khambhupati A, Udgire M, Paul D, Mathur S. Preliminary phytochemical studies  
553 and evaluation of antibacterial activity of *Psoralea corylifolia* seed extract. *IJMRR*. 2014; 2:  
554 095-101.
- 555 29. Gursalkar T, Bajaj A, Jain D. Cyclodextrin based nanosponges for pharmaceutical use: A  
556 review. *Acta Pharm*. 2013;63:335-58.
- 557 30. Loftsson T, Brewster M. Pharmaceutical applications of cyclodextrins: drug solubilisation  
558 and stabilization. *J Pharm Pharmacol*. 1996; 85: 1017-25.
- 559 31. Trotta F, Tumiatti V, Cavalli R, Roggero C, Mognetti B, Berta G. Cyclodextrin-based  
560 nanosponges as a vehicle for antitumoral drugs. WO2009/003656 A1; 2009.
- 561 32. <http://www.inchem.org/documents/sids/sids/102090.pdf> (assessed on Dec, 2016)
- 562 33. Sharma R, Pathak K. Polymeric nanosponges as an alternative carrier for improved retention  
563 of econazole nitrate onto the skin through topical hydrogel formulation. *Pharm. Dev.*  
564 *Technol*. 2011;16(4):367-76.
- 565 34. Anandam S, Selvamuthukumar S. Optimization of microwave-assisted synthesis of  
566 cyclodextrin nanosponges using response surface methodology. *J Porous Mat*. 2014;  
567 21(6):1015-23.
- 568 35. Ferro M, Castiglione F, Punta C, Melone L, Panzeri W, Rossi B, Trotta F, Mele A. Anomalous  
569 diffusion of Ibuprofen in cyclodextrin nanosponge hydrogels: an HRMAS NMR study.  
570 *Beilstein J Org Chem*. 2014;10(1):2715-23.
- 571 36. Selvamuthukumar S, Anandam S, Krishnamoorthy K, Rajappan M. Nanosponges: A novel  
572 class of drug delivery system-review. *J Pharm Pharm Sci*. 2012; 15(1):103-11.
- 573 37. Aldawsari HM, Badr-Eldin SM, Labib GS, El-Kamel AH. Design and formulation of a topical  
574 hydrogel integrating lemongrass-loaded nanosponges with an enhanced antifungal effect: in  
575 vitro/in vivo evaluation. *Int J Nanomedicine*. 2015;10:893-902.
- 576 38. Olteanu AA, Aramă CC, Radu C, Mihăescu C, Monciu CM. Effect of  $\beta$ -cyclodextrins based  
577 nanosponges on the solubility of lipophilic pharmacological active substances (repaglinide).  
578 *J Incl Phenom Macrocycl Chem*. 2014; 80: 17-24.
- 579 39. Carlotti ME, Sapino S, Vione D, Pelizzetti E, Trotta M. Photostability of Trolox in  
580 Water/Ethanol, Water, and Oramix CG 110 in the Absence and in the Presence of TiO<sub>2</sub>. *J*  
581 *Disper Sci Technol*. 2004; 25: 193-207.
- 582 40. Carlotti ME, Sapino S, Vione D, Minero C, Peira E, Trotta M. Study on the photodegradation  
583 of salicylic acid in different vehicles in the absence and in the presence of TiO<sub>2</sub>. *J Disper Sci*  
584 *Technol*. 2007; 28: 805-818.